Geomechanics and Engineering, *Vol. 42, No. 2 (2025) 81-92*
https://doi.org/10.12989/gae.2025.42.2.081

A novel soil breakage index incorporating particle surface energy change and its application to predict the evolution of PSD during triaxial shearing

Feng Gao[1a], Jungao Zhu*[1], Tao Wang[2b], Long Wang[3c], Fulong Ma[4d] and Qixun Luo[4e]

[1]*Key Laboratory of Ministry of Education for Geomechanics and Embankment Engineering, Hohai University, Nanjing, Jiangsu 210098, China*
[2]*School of Earth Sciences and Engineering, Nanjing University, 163 Xianlin Road, Nanjing 210023, China*
[3]*Huaneng Lancang River Hydropower Inc., Kunming, Yunnan 650214, China*
[4]*Chengdu Engineering Corporation Limited, Power China. Chengdu, Sichuan 610072, China*

(*Received November 11, 2024, Revised June 12, 2025, Accepted June 25, 2025*)

Abstract. Particle breakage is an unavoidable phenomenon in granular soils, fundamentally representing the transformation of deformation energy into the surface energy. This paper, based on fractal theory, derives analytical solution for the breakage index incorporating particle surface energy change. It compares this novel breakage index with the established breakage indices. Qualitatively, the novel breakage index demonstrates similar trends to the established breakage indices. Quantitatively, the established breakage indices tend to overestimate the degree of particle breakage. Utilizing the novel breakage index, a particle breakage model and a particle size distribution (PSD) evolution model were suggested and validated. The surface morphology of the particle breakage model is found to conform to a hyperbolic paraboloid. The PSD evolution model accurately reflects the evolution trends of granular soils. Notably, quartz sand exhibits relatively high prediction accuracy, while the prediction accuracy for rockfill and carbonate sand is slightly limited.

Keywords: fractal theory; particle breakage index; particle breakage model; particle surface energy; PSD evolution model

1. Introduction

Granular soils, such as rockfill, quartz sand, and carbonate sand, are prevalent in geotechnical engineering applications, serving as foundation soils beneath pile tips (Li *et al.* 2024), filter materials for earth-rock dams (Nhu *et al.* 2024), railway ballast (Kiana *et al.* 2018), and in island reef engineering (Wang *et al.* 2020). With the rapid advancement of deep pile and high earth-rock dam construction, particle breakage has emerged as a significant and inevitable concern (Ma *et al.* 2021). Particle breakage often induces alterations in the PSD of the soil (Zhou and Zhang 2016), constrains dilatancy (Wang *et al.* 2024), diminishes peak strength, and ultimately results in extensive deformations and structural failure. Accurately quantifying the extent of particle breakage is pivotal for comprehensively assessing its impact on the mechanical behavior of soils (Guo *et al.* 2024, Wang *et al.* 2024a, Wang *et al.* 2025).

The breakage indices proposed based on changes in the PSD can be primarily categorized into three groups. The first group is predicated on alterations in characteristic particle size or single PSD index (Lee and Farhoomand 1967, Lade *et al.* 1996, Nakata *et al.* 1999); the second group focuses on variations in particle group content (Marsal 1967, Xiao *et al.* 2021); the third group revolves around breakage potential (Hardin 1985, Indraratna *et al.* 2005, Einav 2007, Muir Wood and Maeda 2008). The process of particle breakage fundamentally entails the conversion of deformation energy into surface energy (McDowell *et al.* 1996, McDowell and Bolton 1998). However, prevailing global breakage indices are derived by computing the ratio of areas between different states (initial state, current state, ultimate state) of the PSD in the P-log$d$ coordinate system via integration, disregarding alterations in particle surface energy. McDowell *et al.* (1996) have explored the influence of particle breakage on the mechanical behavior of granular soils by considering changes in particle surface energy, they have yet to propose a breakage index that accounts for such variation.

According to the definition of the breakage index, the most direct approach to its determination is through particle sieving to obtain the PSD. However, the triaxial test is procedural, and sieving the particles would necessitate sample dismantling, thus terminating the test prematurely. Consequently, Shi *et al.* (2022) have developed mathematical models that depict the relationship between the particle breakage index and stress-strain to predict the extent of breakage. Salim and Indraratna (2004) established a correlation between the breakage index and mean effective stress, as well as shear strain, based on triaxial

*Corresponding author, Professor
E-mail: zhujungao@hhu.edu.com
[a]Ph.D. Student
[b]Ph.D.
[c]Ph.D.
[d]Ph.D.
[e]Senior Engineer

ISSN: 2005-307X (Print), 2092-6219 (Online)

tests conducted on rockfill. Nakata *et al.* (1999) established a relationship between the breakage index and the maximum value of mean normal effective principal stress, drawing from triaxial tests performed on sand. Zeng and Liu (2023) established a particle breakage model applicable to calcareous sand and indicated that the parameter A in their model was influenced mainly by the mineral composition and particle morphology of coral sand. Presently, most existing particle breakage models have been validated using only a single type of granular soil, and their applicability to other granular materials remains uncertain.

Moreover, gradation is an important parameter of soil (Shi *et al*. 2024, Gao *et al.* 2025, Shi *et al*. 2025), with particle breakage and PSD evolution invariably occur concurrently. Jia *et al.* (2017) conducted a comprehensive review of prior studies and noted significant disparities in the evaluation of particle breakage, often overlooking the dynamic evolution process of breakage and focusing solely on its conclusion at the end of the test. Consequently, numerous researchers have undertaken triaxial shear tests on various materials such as rockfill (Jia *et al.* 2017, Guo *et al.* 2019), quartz sand (Yu 2017, Chen *et al.* 2023), and carbonate sand (Yu 2018, Zhang *et al.* 2020), subjecting them to diverse confining pressure and shear strain to elucidate the ongoing evolution of particle breakage. Similar to particle breakage model, most existing PSD evolution models have been validated using only a single type of granular soil, and their applicability to other granular materials remains uncertain.

In summary, the current particle breakage indices lack a connection to particle surface energy change, and the applicability of existing particle breakage models and PSD evolution models to various types of granular soils is unclear. To address these gaps, this paper derives analytical solution for the breakage index incorporating particle surface energy change based on fractal theory. It examines the disparities between the novel breakage index and commonly breakage indices. Employing the novel breakage index as a foundation, empirical formulas are developed for a particle breakage model and a PSD evolution model tailored to the triaxial shearing across various granular soils. Subsequently, the validity of these two models is assessed using existing literature data.

2. Particle breakage index

2.1 Overview of breakage index

Particle breakage pertains to the fracture or abrasion phenomenon ensuing from external forces surpassing the particles' failure strength, leading to the fragmentation of parent particles into multiple daughter particles. It constitutes an ongoing and dynamic process, particularly evident in the evolution of PSD for particle aggregates. Numerous researchers have delineated various breakage indices grounded in PSD to quantify the extent of particle breakage. In this paper, existing breakage indices are systematically classified and presented in Table 1, while the definitions of pertinent physical quantities are illustrated in Fig. 1.

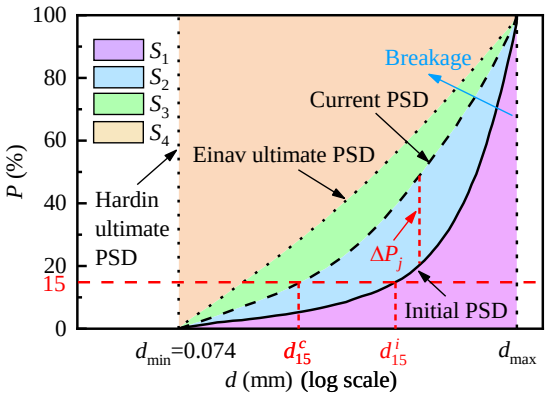

Fig. 1 Schematic diagram of PSD breakage evolution

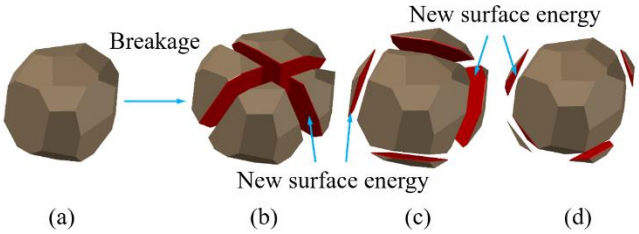

Fig. 2 Increase in surface energy resulting from particle breakage: (a) Parent particle, (b) Fracture, (c) Attrition and (d) Abrasion

Breakage indices defined based on characteristic particle size or single PSD index offer simplicity in calculation. However, they solely track alterations in specific characteristic particle sizes or individual PSD indices, thus failing to provide a comprehensive assessment of the overall breakage extent within the sample. In contrast, breakage indices grounded in particle group content mitigate these limitations to some extent. Yet, the precision of breakage degree measurement is intricately tied to the breadth of each particle group, with accuracy diminishing as the group range widens. Breakage indices formulated based on breakage potential exhibit the capability to encompass particle breakage across all sizes, making them a preferred choice for many researchers in evaluating breakage degree. Nonetheless, breakage potential is an artificially defined metric lacking clear physical significance.

In the realm of comminution engineering, three prominent theories of breakage energy are recognized. Among them is Von Rittinger's surface area theory (Von Rittinger 1867), which posits that particle breakage accompanies an increase in surface area. This theory suggests that the energy expended per unit mass of material for breakage is directly proportional to the augmented surface area. Fig. 2 depicts three modes of particle breakage: fracture, attrition, and abrasion. Irrespective of the mode of breakage, the underlying principle remains consistent: particles are subjected to forces, absorb energy, and undergo breakage upon reaching a specific threshold. This process entails the conversion of deformation energy into surface energy (McDowell *et al.* 1996). Consequently, from a theoretical standpoint, it is more apt to employ

Table 1 Existing particle breakage indices

Reference	Definition	Range
Lee and Farhoomand (1967)	$B_{15}=d_{15}^{i}/d_{15}^{c}$	>1
Lade *et al.* (1996)	$B_{10}=1-d_{10}^{c}/d_{10}^{i}$	0~1
Nakata *et al.* (1999)	$B_f=1-R_0/100$	0~1
Marsal (1967)	$B_g=\Sigma\Delta P_j$	>0
Xiao *et al.* (2021)	$B_N^*=\frac{M^c-M^i}{M^u-M^i}$	0~1
Hardin (1985)	$B_r^H=\frac{B_t}{B_p}=\frac{S_2}{S_2+S_3+S_4}$	0~1
Indraratna *et al.* (2005)	$B_r^I=BBI=\frac{E}{E+F}$	0~1
Einav (2007)	$B_r^E=\frac{S_2}{S_2+S_3}$	0~1
Muir Wood and Maeda (2008)	$B_r^W=I_G=\frac{S_1+S_2}{S_1+S_2+S_3}$	0~1

Note: d_{15} is the particle size at which the fine particle content is 15%; superscripts *i*, *c*, and *u* are the initial state, the current state (the end of the experiment is one of them), and the ultimate state; R_0 is the percentage of the minimum particle size in the initial state corresponding to the PSD at the end of the experiment; ΔP_j is the positive value of the percentage difference in the content of a certain particle group before and after breakage; M is the sum of the cumulative percentage content of each particle group in a certain state; B_p is the breakage potential; B_t is total breakage; E is the area enclosed by the initial PSD and the current PSD; F is the area enclosed by the current PSD and any arbitrary straight line boundary considering the maximum breakage amount; S_1, S_2, S_3 and S_4 are shown in Fig. 1.

changes in particle surface energy to gauge the degree of particle breakage.

2.1 Breakage index incorporating particle surface energy change

The fractal theory offers a simple and distinctive parameterization for characterizing the PSD of soils, and its application has been widespread in the investigation of particle breakage within granular materials, encompassing sand (McDowell and Daniell 2001), carbonate sand (Li *et al.* 2022), and rockfill (Guo and Chen 2022). Typically, the fractal gradation equation can be expressed as

$$P(d)=\left(\frac{d}{d_{\max}}\right)^{3-D} \tag{1}$$

Where P is the cumulative percentage content, d is the particle size, $d_{\max}$ is the maximum particle size, and D is the fractal dimension, governing the shape of the PSD.

Taking the derivative of d, the probability density distribution function of P with respect to d can be expressed as

$$p(d)=P'(d)=(3-D)d_{\max}^{D-3}d^{2-D} \tag{2}$$

Assuming spherical particle morphology, the surface area of the particle aggregate with a particle size d is given by

$$S_s=\frac{m_a p(d)}{m_d}s_d \tag{3}$$

Where m_a is the total mass of sample, m_d is the mass of a single spherical particle with diameter d, and s_d is the surface area of a single spherical particle with diameter d.

However, natural particles frequently display irregular shapes rather than being perfectly spherical. Assuming spherical particles would underestimate the surface area for an equivalent volume. Sphericity measures how closely an object resembles a sphere, ranging from 0 (highly angular) to 1 (perfectly spherical) (Wadell 1932). It is defined as the ratio of the surface area of a sphere with the same volume as the particle to the actual surface area of the particle. Mathematically, sphericity can be expressed as

$$\psi=\frac{\sqrt[3]{36\pi V^2}}{A} \tag{4}$$

Where V and A represent volume and surface area of the naturally occurring particle, respectively.

For the naturally occurring particle , the surface area of the particle aggregate with a particle size d is given by

$$S_n=\frac{S_s}{\psi}=\frac{m_a p(d)}{\psi m_d}s_d \tag{5}$$

By integrating Eq. (5) over the entire particle size range, the total surface area of the particles in the sample can be determined. It is important to note that there is currently no consensus on the minimum particle size following breakage of granular soils. Hardin (1985) once assumed that particles with a size smaller than 0.074mm no longer break, and this assumption has been widely adopted. Similarly, this paper adopts $d_{\min}$=0.074 mm. Hence, the total surface area of the particles in the sample comprises two components: (1) the surface area of the particle aggregates with particle sizes ranging from ($d_{\min}$, $d_{\max}$); (2) the surface area of particle

aggregates with sizes smaller than $d_{\min}$, which are replaced by particles with a diameter of $d_{\min}$ on an equal-mass basis. The total surface area of the particle in the sample is

$$S = \int_{d_{\min}}^{d_{\max}} \frac{m_a p(d)}{\psi m_d} s_d \, \mathrm{d}d + \frac{m_a P(d_{\min})}{\psi m_{d_{\min}}} s_{d_{\min}} \tag{6}$$

Where $d_{\min}$ is the minimum particle size, $P(d_{\min})$ is the cumulative percentage content of particles with sizes smaller than $d_{\min}$, $m_{d_{\min}}$ is the mass of a single spherical particle with diameter $d_{\min}$, and $s_{d_{\min}}$ is the surface area of a single spherical particle with diameter $d_{\min}$.

By solving the integral of Eq. (6), the total surface area of the particles in the sample is obtained as

$$S = \frac{6m_a}{\psi\rho}\left[\frac{(3-D)d_{\max}^{D-3}}{(2-D)}\left(d_{\max}^{2-D} - d_{\min}^{2-D}\right) + d_{\min}^{2-D}\cdot d_{\max}^{D-3}\right] \tag{7}$$

Where ρ is the density of granular soil.

McDowell (1996) considered surface energy to be the product of surface free energy and surface area. The total surface energy of the particles in the sample can be represented as

$$E_s = \Gamma S = \frac{6\Gamma m_a}{\psi\rho}\left[\frac{(3-D)d_{\max}^{D-3}}{(2-D)}\left(d_{\max}^{2-D} - d_{\min}^{2-D}\right) + d_{\min}^{2-D}\cdot d_{\max}^{D-3}\right] \tag{8}$$

Where Γ is the surface free energy.

At the beginning of particle breakage, the initial PSD corresponds to an initial surface energy. As particle breakage continues, the surface energy of the particles gradually increases until reaching a ultimate PSD, at which point particle breakage ceases and a maximum surface energy is attained. Therefore, the breakage index incorporating particle surface energy can be defined as

$$B_s = \frac{E_s^c - E_s^i}{E_s^u - E_s^i} \tag{9}$$

Where E_s^i, E_s^c, and E_s^u are the surface energy of the sample in the initial, current, and ultimate state, respectively. According to Eq. (8), with other parameters being constant, the surface energy can be determined once the PSD of the sample is obtained. The PSD in the initial and current states can be readily obtained through sieve tests. However, consensus is lacking regarding the ultimate state. Currently, two predominant approaches exist: (1) the minimum particle size theory proposed by Hardin (1985), where all particles are assumed to break down to a minimum diameter of 0.074 mm; (2) the concept of ultimate fractal dimension suggested by Einav (2007). Prior research indicates that under extremely high stress or shear strain, an ultimate PSD exists, adhering to a fractal distribution (Coop *et al.* 2004). When the fractal dimension of granular soil is known, researchers tend to prefer the Einav's ultimate state. In this scenario, the analytical solution for the particle breakage index is

$$B_s^E = \frac{f(D^c) - f(D^i)}{f(D^u) - f(D^i)} \tag{10}$$

Function $f(D)$ is defined as

$$f(D) = \frac{(3-D)d_{\max}^{D-3}}{2-D}(d_{\max}^{2-D} - d_{\min}^{2-D}) + d_{\min}^{2-D}d_{\max}^{D-3} \tag{11}$$

While the Einav's ultimate state theory is more comprehensive, obtaining the ultimate fractal dimension under commonly available test conditions (such as one-dimensional compression, simple shear, and triaxial shear) is challenging. Therefore, for practical purposes, the Hardin's ultimate state is introduced, where all particles are assumed to break down to a size of 0.074 mm. Under this assumption, the surface energy of the sample is

$$E_s^{uH} = \frac{\Gamma m_a}{\psi m_{d_{\min}}} s_{d_{\min}} \tag{12}$$

By substituting Eq. (12) into Eq. (9) and combining it with Eq. (10), the analytical solution for the particle breakage index under the Hardin's ultimate state can be derived as

$$B_s^H = \frac{f(D^c) - f(D^i)}{\frac{1}{d_{\min}} - f(D^i)} \tag{13}$$

According to Eqs. (10) and (13), the particle breakage index incorporating particle surface energy depends solely on the current fractal dimension D^c, with other parameters being constant. The particle breakage process mathematically corresponds to the transition of the current fractal dimension D^c from the initial fractal dimension D^i to the ultimate fractal dimension D^u, which corresponds to the breakage index changing from 0 to 1.

2.3 Relationship between breakage index and input energy

Particle breakage is a process wherein the work exerted by external loads is transformed into the surface energy of newly formed particles (McDowell *et al.* 1996). An improved particle breakage index should have a one-to-one correspondence with the breakage energy during breakage.

However, existing breakage indices and breakage energy do not always align directly.

As depicted in Fig. 3, for a sample with a known initial PSD, under the influence of external loads, the PSD may evolve into either current PSD 1 or current PSD 2 after breakage. For example, using the Hardin's breakage index, for the current PSD 1, Hardin's breakage index $B_r^H = (S_5 + S_7)/B_p$. For the current PSD 2, $B_r^H = (S_5 + S_6)/B_p$. If S_5=S_6, it means that the particle breakage indices for both current PSD 1 and current PSD 2 are equal, implying equal of breakage energy. However, it is evident that the content of fine particles in the current PSD 1 is greater than that in the current PSD 2. More content of fine particles necessitates the absorption of more energy. Consequently, the breakage index for the current PSD 1 should exceed that for the current PSD 2, a distinction not reflected by the breakage indices proposed by Hardin. Einav's breakage index similarly fails to reflect this. In

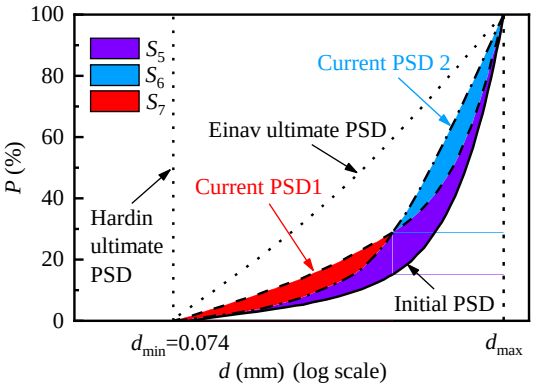

Fig. 3 Two forms of current PSD

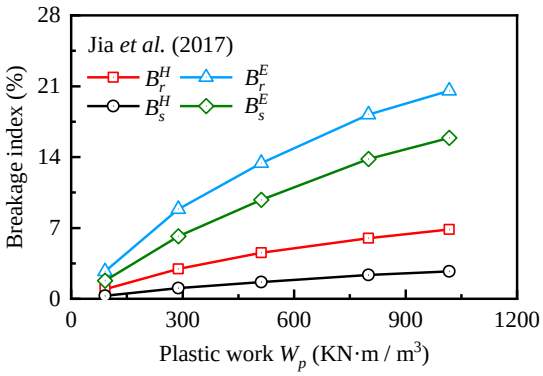

Fig. 4 Relationship between breakage indices and plasti work

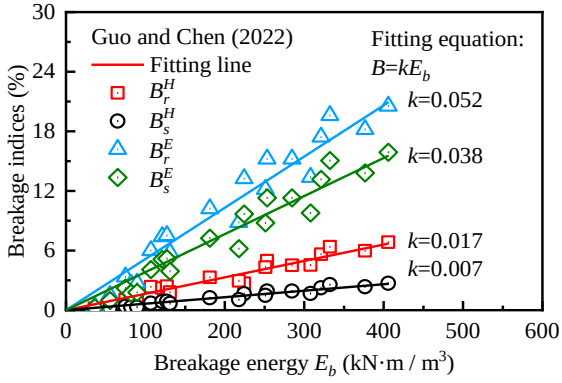

Fig. 5 Relationship between breakage indices and breakage energy

contrast, the breakage index incorporating particle surface energy change establishes a mathematical relationship between the breakage index and particle surface energy from an analytical perspective, fundamentally addressing the issue of the breakage index not corresponding directly to breakage energy.

The total input energy can be partitioned into two components: elastic work and plastic work, with plastic work being the primary contributor to particle breakage. Many researchers have investigated the relationship between the Hardin's or Einav's particle breakage index and plastic work (Jia *et al.* 2017). Plastic work is often expressed as

$$W_p = \int p d\varepsilon_v^p + q d\varepsilon_s^p \tag{14}$$

Where p is the mean effective stress, q is the deviatoric stress, ε_v^p is the plastic volumetric strain, and ε_s^p is the plastic shear strain.

The proposed breakage indices were verified using the trend consistency principle by comparing them with the Hardin's and Einav's breakage indices respectively. Triaxial test data of Gushui rockfill conducted by Jia *et al.* (2017) were utilized as an example. Fig. 4 illustrates the relationship between breakage indices and plastic work under a confining pressure of 2000 kPa and shear strains of 1.85%, 4.55%, 7.26%, 10.75%, and 13.76%. The ultimate fractal dimension of the rockfill is assumed to be 2.7 (Yang and Juo 2001). Qualitatively, the proposed particle breakage indices exhibit a hyperbolic form similar to existing particle breakage indices, affirming the rationality of the proposed breakage indices.

Quantitatively, during the initial loading of the sample at a shear strain of 1.85%, minimal differences are observed between the proposed breakage indices and existing breakage indices. However, with continued input of plastic work, the disparities between these indices become increasingly significant. Since the proposed particle breakage index corresponds to the additional surface energy from an analytical perspective, it means that existing breakage indices overestimate the additional surface energy, thus overestimating the degree of particle breakage. As plastic work increases, the overestimation of breakage degree by existing indices becomes more significant. When the shear strain reaches 13.76%, Hardin's breakage index overestimates by 152.9%, and Einav's breakage index overestimates by 29.2%. This error is not negligible.

The particle breakage index should exhibit a linear relationship with breakage energy theoretically (Von Rittinger 1867). Guo and Chen (2022) computed specific values of breakage energy based on triaxial tests conducted by Jia *et al.* (2017) on Gushui rockfill. Utilizing data from Guo and Chen (2022), Fig. 5 depicts and fits the relationship between various breakage indices and breakage energy using scatter points. It reveals that a straight-line fit effectively describes the relationship between breakage indices and breakage energy in Gushui rockfill. This linear relationship can be expressed as

$$B = kE_b \tag{15}$$

Where B is a generic term for the breakage index, k is the fitting slope and can be regarded as a material parameter, and E_b is the breakage energy. As B is a dimensionless quantity, the unit of k is (m^3 / kN m).

In Fig. 5, a linear relationship is evident between the four breakage indices and the breakage energy, indicating the rationality of these indices to a certain extent. Fig. 5 incorporates data from experiments conducted by Jia *et al.* (2017) , spanning the entire process from initial shearing to failure of Gushui rockfill under four confining pressures of

500, 1000, 1500, and 2000 kPa. It can be observed that under different confining pressures, existing particle breakage indices always overestimate the degree of particle breakage. The extent of overestimation can be quantitatively expressed as

$$O = \Delta k E_b \tag{16}$$

3. Particle breakage model

3.1 Establishment of the model

During the loading process, particle breakage occurs as a result of stress and strain. This allows for the establishment of a mathematical relationship between particle breakage and stress-strain behavior. Jia *et al.* (2017) and Guo *et al.* (2019) conducted a series of triaxial shear tests on rockfill, while other researchers have pursued similar investigations on quartz sand (Yu 2017, Chen *et al.* 2023) and carbonate sand (Yu 2018, Zhang *et al.* 2020). The outcomes underscore that particle breakage results from the combined influence of mean effective stress p and shear strain ε_s. Despite these findings, a particle breakage model encapsulating the mathematical relationship between breakage index B_s^E, p and ε_s for rockfill, quartz sand, and carbonate sand remains elusive. Hence, leveraging existing research data, this paper analyzes the association between B_s^E, p and ε_s. Subsequently, an empirical particle breakage model applicable to rockfill, quartz sand, and carbonate sand is established. The model can be expressed as

$$B_s^E = m(p / p_a - a)(\varepsilon_s - b)^n \tag{17}$$

Where m, a, b, and n are fitting parameters, which are dimensionless quantities, P_a is atmospheric pressure, typically taken as 101 kPa.

Considering the theoretical soundness, the ultimate fractal dimension presumed by Einav (2007) is adopted as a reference for the ultimate state of breakage. Eq. (17) is found to conform to a hyperbolic paraboloid in the $B_s^E - p - \varepsilon_s$ three-dimensional coordinate system. In the subsequent analysis, Eq. (17) will be validated utilizing existing data from triaxial shearing of rockfill, quartz sand, and carbonate sand under varying confining pressures, as detailed in Table 2. It is noteworthy that the ultimate fractal dimension for rockfill is assumed as 2.7 (Yang and Juo 2001), for quartz sand it is 2.47 (Xiao *et al.* 2018), and for carbonate sand it is 2.63 (Xiao *et al.* 2018).

3.2 Model validation

Fig. 6 depicts the relationship between the breakage index, mean effective stress, and shear strain for two types of rockfill under varying confining pressures. Fig. 6(a) and 6(b) present similar spatial surface morphologies, showcasing different perspectives of the data. From Fig. 6(b), it is evident that as mean effective stress or shear strain increases, the breakage index also rises, with both mean effective stress and shear strain exerting an influence on particle breakage following a hyperbolic paraboloid pattern. When mean effective stress is high and shear strain is low, the degree of particle breakage remains relatively low. Similarly, when mean effective stress is low and shear strain is high, particle breakage is also low. Notably, significant particle breakage occurs only when mean effective stress reaches a certain threshold, increasing shear strain. This phenomenon stems from the compression of granular soil samples, leading to denser particles and increased coordination, forming protective force chains (Wang *et al.* 2024b). Consequently, breakage during isotropic consolidation of samples can be disregarded. Additionally, when mean effective stress is low and shear strain develops, particles are more prone to rolling under shear stress due to the minimal normal force they receive, rather than breaking. Hence, significant particle breakage occurs only when mean effective stress reaches a critical value and shear strain is subsequently generated. This observation is consistent with the findings of Wang *et al.* (2020) , who studied the breakage mechanism of carbonate sand and concluded that particle breakage results from the coupling effect of compression and shear mechanisms.

Table 2 Data used for validating the particle breakage model

Reference	Material	d_{max}(mm)	D^{μ}
Jia *et al.* (2017)	Rockfill	60	2.7
Guo *et al.* (2019)	Rockfill	20	2.7
Yu (2017)	Quartz sand	0.85	2.47
Chen *et al.* (2023)	Quartz sand	1	2.47
Zhang *et al.* (2020)	Carbonate sand	2	2.63
Yu (2018)	Carbonate sand	2	2.63

Subsequently, a pertinent question emerges: which factor, mean effective stress (compression) or shear strain (shear), contributes more significantly to particle breakage? Examining Fig. 6, it is evident that the particle breakage model proposed in this paper, encapsulated by Eq. (17), adeptly fits the relationship between the particle breakage index and both mean effective stress and shear strain, yielding high R^2 values of up to 0.97. Given known values of mean effective stress and shear strain, one can readily substitute them into Eq. (17) to derive a specific breakage index and subsequently compare its magnitude.

Figs. 7 and 8 illustrate the relationship between the breakage index, mean effective stress, and shear strain, for two types of quartz sands and carbonate sands, respectively, depicted from two perspectives. Notably, Eq. (17) demonstrates applicability to quartz sands and carbonate sands, yielding even greater accuracy with an R^2 value of 0.99. The breakage patterns observed in quartz sands and carbonate sands are largely consistent with those observed in rockfill, also exhibiting a hyperbolic paraboloid trend.

Fig. 9 compares the predicted breakage index calculated using Eq. (17) with the experimental (actual) values for rockfill, quartz sand, and carbonate sand. It is evident that the data points are closely distributed within a narrow range along a line with a slope of 1, signifying the high accuracy of the particle breakage model proposed in this paper.

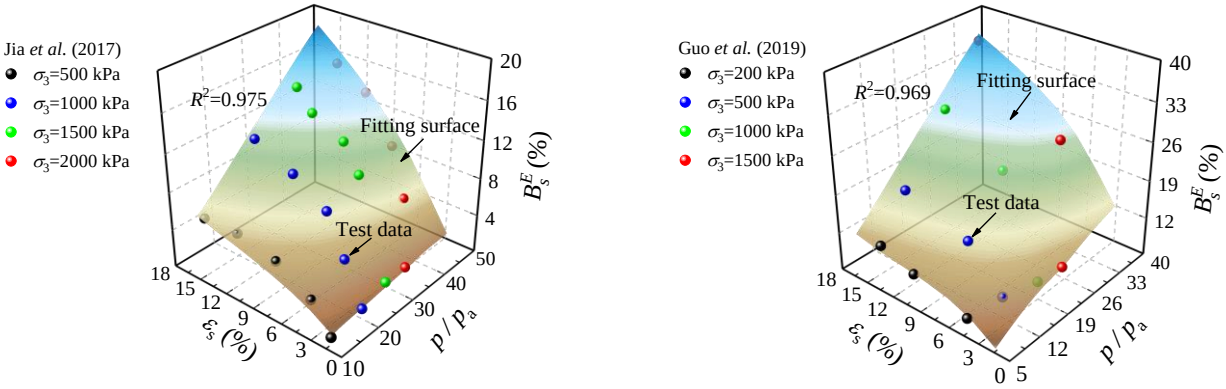

(a) m=0.0776, a=-2.3052, b=1.4084, n=0.6081 (b) m=0.4209, a=-9.6443, b=1.2407, n=0.2509

Fig. 6 Relationship between the breakage index and stress-strain of rockfills

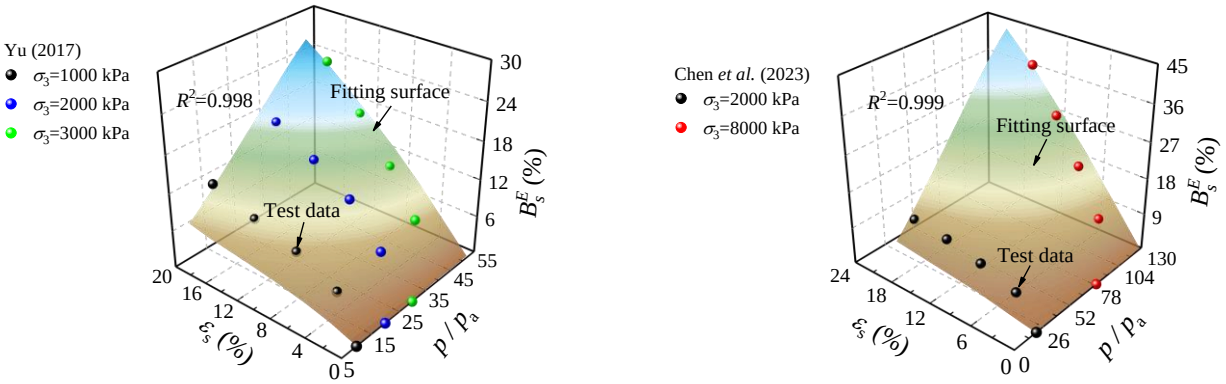

(a) m=0.0441, a=-1.6620, b=-0.0095, n=0.8001 (b) m=0.0350, a=8.0662, b=1.1240, n=0.7850

Fig. 7 Relationship between the breakage index and stress-strain of quartz sands

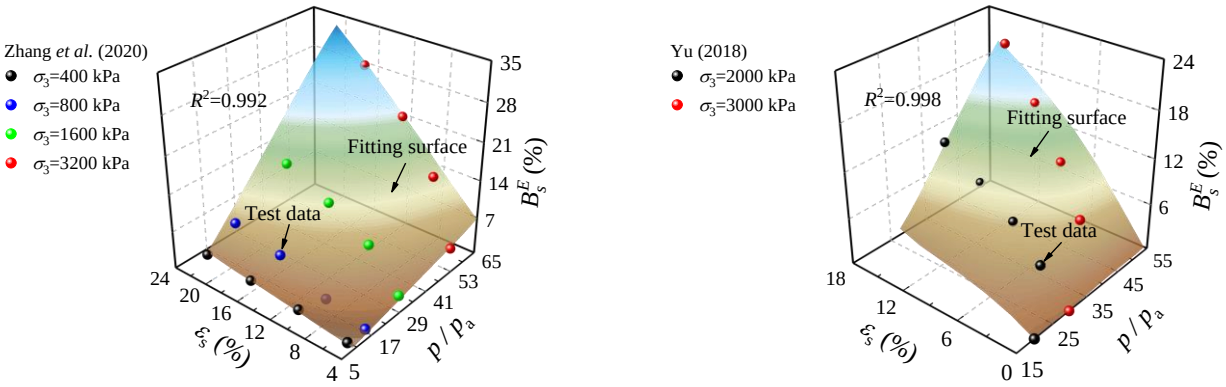

(a) m=0.0776, a=-2.3052, b=1.4084, n=0.6081 (b) m=0.4209, a=-9.6443, b=1.2407, n=0.2509

Fig. 8 Relationship between the breakage index and stress-strain of carbonate sands

4. PSD evolution model

The evolution of the PSD and particle breakage occur simultaneously and are inseparable processes. Once the fractal dimension D^c of the current PSD is determined, the current PSD is also fixed. The PSD evolution model can be conceptualized as a mathematical relationship between the current fractal dimension, mean effective stress, and shear strain. Fig. 10 illustrates the relationship between the current fractal dimension and the breakage index during the triaxial shear process for rockfill, quartz sand, and carbonate sand. It is observed that a linear relationship exists between D^c and B_s^E, which can be expressed as

$$D^c = \alpha B_s^E + \beta \tag{18}$$

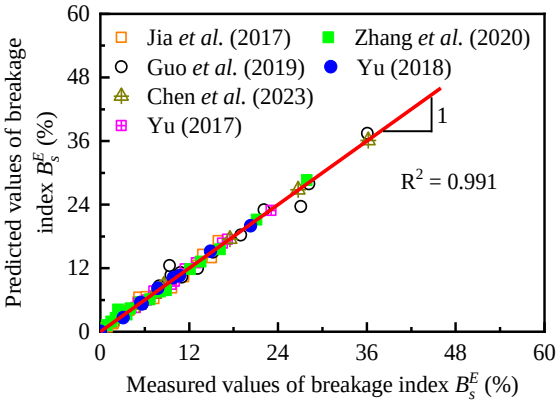

Fig. 9 Linear regression analyses between the fitted data and measured data of B_s^E

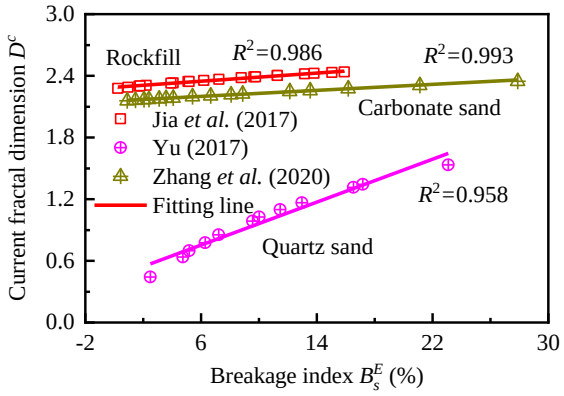

Fig. 10 Relationship between D^c and B_s^E

Where α and β are the fitting parameters. The best- fit parameters are shown in Table 3.

By combining Eq. (17) and (18), a mathematical relation ship between the current fractal dimension D^c, p, and ε_s can be derived and expressed as

$$D^c = \alpha m(p / p_0 - a)(\varepsilon_s - b)^n + \beta \quad (19)$$

Thus far, this paper has completed the derivation of the analytical solution for the breakage index incorporating particle surface energy change, established the relationship between the breakage index and stress-strain (particle breakage model), and finally obtained the mathematical expression between the current fractal dimension and stress-strain (PSD evolution model).

To test the predictive performance of the PSD evolution model, Fig. 11 compares the predicted PSD based on Eq. (19) with the actual measured PSD at high confining pressure for rockfill, quartz sand, and carbonate sand during the triaxial shearing. It can be observed that the predicted values can reflect the trend of PSD changes. For quartz sand, the prediction accuracy is relatively high. However, for rockfill and carbonate sand, the prediction accuracy is slightly weaker. This is related to the inherent limitations of the fractal gradation equation, which will be discussed in detail later.

Table 3 The best-fit parameters

Reference	Material	α	β	R^2
Jia *et al.* (2017)	Rockfill	0.010	2.287	0.986
Yu (2017)	Quartz sand	0.052	0.439	0.993
Zhang *et al.* (2020)	Carbonate sand	0.007	2.157	0.958

A robust PSD evolution model should accurately predict the PSD changes under various stress conditions. Fig. 12 presents the predicted evolution of PSD under low confining pressure. It is observed that the predictive performance of the PSD evolution model is similar to that under high confining pressure, indicating the model's applicability to predicting the particle size distribution evolution during triaxial shear processes for various granular soils under different confining pressures.

5. Discussion

Addressing the issue of inaccurate predictions for rockfill and carbonate sand using the PSD evolution model, the first step is to verify the accuracy of the predicted fractal dimension for the current PSD. Fig. 13 compares the fractal dimension predicted by Eq. (19) with the fractal dimension fitted directly from the measured data. It can be observed that the data points

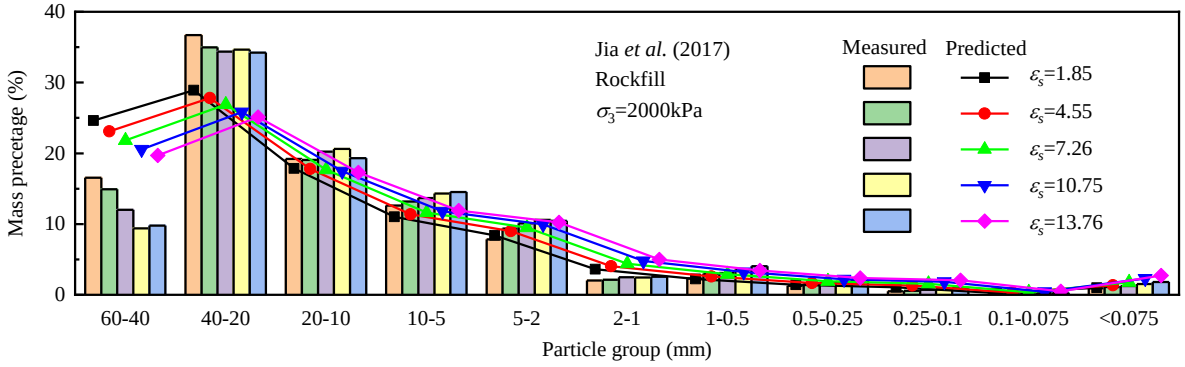

(a) Rockfill

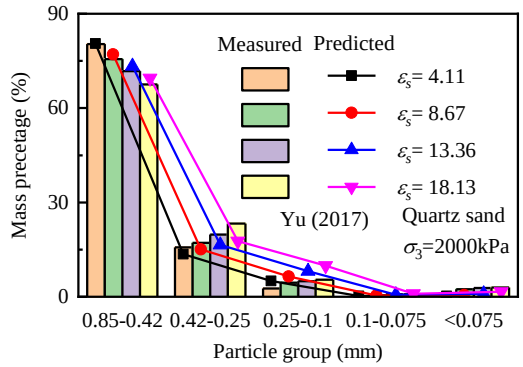

(b) Quart sand

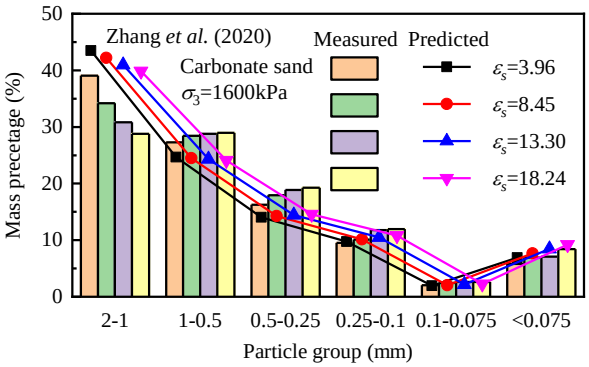

(c) Carbonate sand

Fig. 11 Predicted PSD and measured PSD under high confining pressure

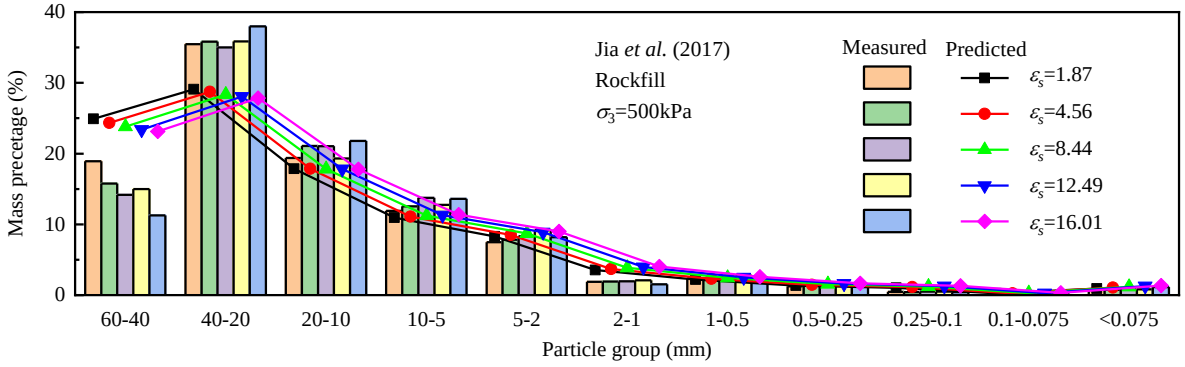

(a) Rockfill

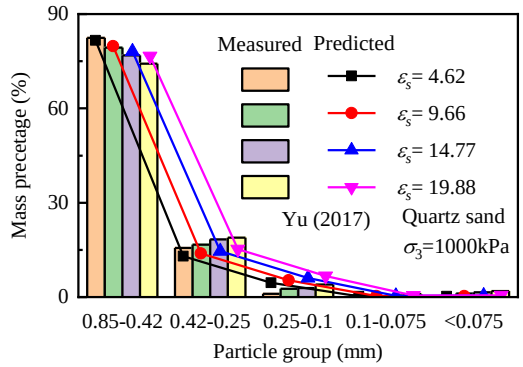

(b) Quart sand

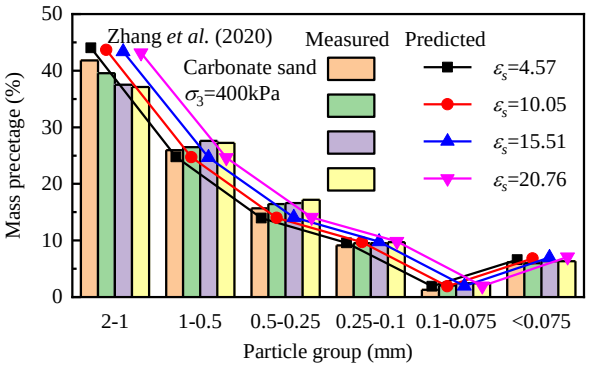

(c) Carbonate sand

Fig. 12 Predicted PSD and measured PSD under low confining pressure

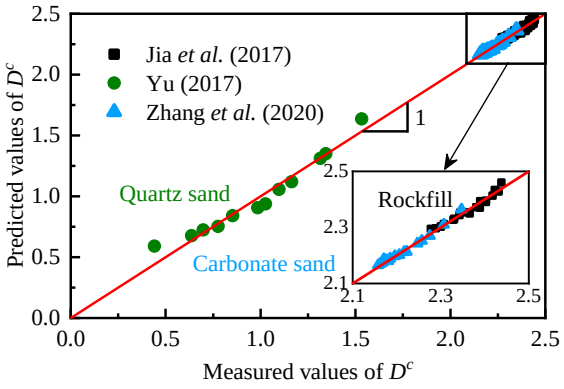

Fig. 13 Linear regression analyses between the fitted data and measured data of D^c

are distributed within a narrow range along a line with a slope of 1, indicating that the predicted fractal dimensions for rockfill and carbonate sand are basically equal to the actual fractal dimensions. Since the prediction of the current fractal dimension is accurate, the problem likely lies in the process of fitting the measured PSD of rockfill and carbonate sand using the fractal gradation equation.

Fig. 14 selects the measured PSD for rockfill (σ_3=2000kPa, ε_s=10.75%), quartz sand (σ_3=2000kPa, ε_s=8.67%), and carbonate sand (σ_3=1600kPa, ε_s=18.24%), and compares the PSD fitted directly using the fractal gradation equation with the measured PSD. It can be observed that the fractal gradation equation has the highest applicability for quartz sand, with an $\Delta P_{\max}$ value of only 1.66%. Carbonate sand follows with an $\Delta P_{\max}$ of 10.72%, and rockfill has the highest $\Delta P_{\max}$ of 11.19%. In other words, there are inherent limitations in using the fractal gradation equation to characterize the PSD of rockfill and carbonate sand.

All the contents of this study are conducted based on the fractal gradation equation. The aforementioned shortcomings belong to the inherent defects of the fractal gradation equation, which cannot be overcome. It is worth mentioning that the authors has previously proposed a dual-parameter gradation equation (Zhu *et al.* 2018) that has a broader applicability than the fractal gradation equation.

This dual-parameter grading equation can be expressed as

$$P = \frac{1}{(1-i)(\frac{d_{\max}}{d})^{\xi} + i} \tag{20}$$

Where i and ξ are the fitting parameters.

However, its drawback lies in the presence of two param eters, which poses difficulties in deriving the breakage inde x incorporating particle surface energy change. Once the an alytical solution for the breakage index is successfully deriv ed using Eq. (20), it is expected to improve the prediction a ccuracy of the PSD evolution model.

In addition, particle shape is considered another key factor that affects the mechanical properties of granular materials (Xiao *et al.* 2022a, Xiao *et al.* 2022b). Typically,

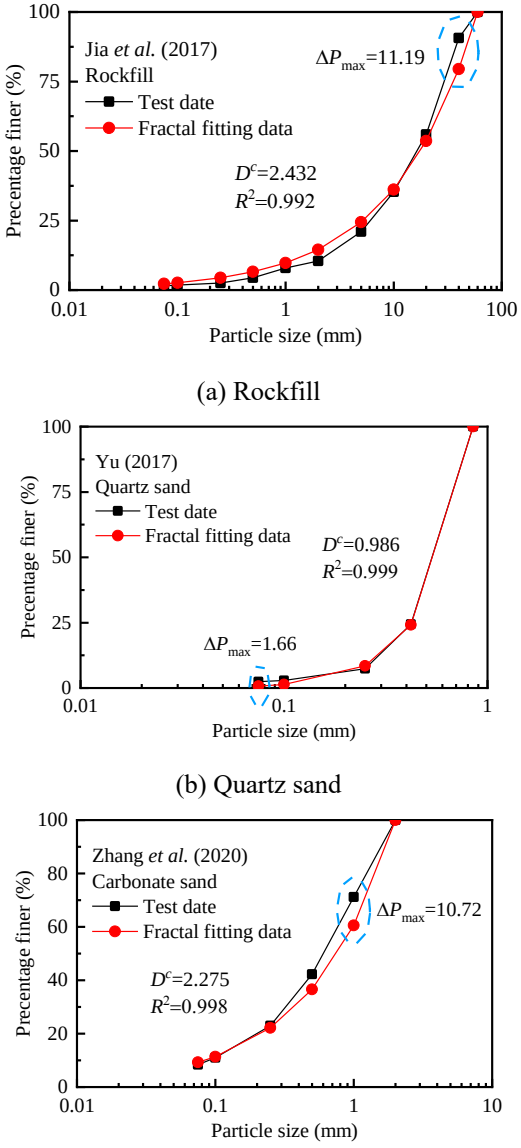

Fig. 14 The applicability of the fractal gradation equation

particles with different shapes tend to exhibit different breakage patterns. For instance, particles with sharp edges tend to break in the pattern shown in Fig. 2(c), while more rounded particles tend to break in the pattern shown in Fig. 2(b). The changes in surface energy associated with these two breakage modes are obviously different. Therefore, the new breakage index holds promise for analyzing the evolution of particle shape during triaxial shearing, but its specific application still requires further research.

6. Conclusions

This paper analyzes the existing evaluation methods and indices for particle breakage. Based on fractal theory, analytical solutions for the breakage indices incorporating particle surface energy change are derived and compared with Hardin's and Einav's breakage indices. Utilizing the

novel breakage index, a particle breakage model and PSD evolution model for granular soils during triaxial shearing are established. The main conclusions can be summarized as follows:

• The new breakage indices have clear physical significance and overcome the limitation of existing breakage indices in quantitatively characterizing breakage energy. During triaxial shearing, Hardin's and Einav's breakage indices tend to overestimate the degree of particle breakage, with the discrepancy increasing progressively with the input energy.

• The particle breakage model was suggested and validated using data from existing literature on rockfill, quartz sand, and carbonate sand. In the $B_s^E - p - \varepsilon_s$ three-dimensional coordinate system, it was found that the surface morphology of the particle breakage model conforms to a hyperbolic paraboloid distribution and particle breakage is the coupling effect of compression and shear mechanisms.

• The PSD evolution model accurately predicts the gradation evolution process of quartz sand. However, there are slight insufficiencies in predicting the PSD evolution of rockfill and carbonate sand. This is mainly due to the inherent limitations of the fractal gradation equation. If a gradation equation with better applicability is utilized, it is expected to improve the accuracy of the PSD evolution model.

Acknowledgments

This work was supported by the Natural Science Foundation of Jiangsu Province (No. BK20230954), the Scientific Project from Huaneng Company Headquarters (HNKJ20-H45), the Yangtze River Water Science Research Joint Fund (U2040221), and the National Natural Science Foundation of China (Grant No. 42407251).

References

Chen, R., Zhao, T., Wu, Z.Y., Hao, D.X., Xue, N. and Yuan, C. (2023), "Experimental investigation on particle breakage behavior of marine silica sand under high-stress triaxial shear", *J. Mar. Sci. Eng.*, **11**(9), 1825. https://doi.org/10.3390/jmse11091825.

Coop, M.R., Sorensen, K.K., Freitas, T.B. and Georgoutsos, G. (2004), "Particle breakage during shearing of a carbonate sand", *Géotechnique.*, **54**(3), 157-163. https://doi.org/10.1680/geot.2004.54.3.157.

Einav, I. (2007), "Breakage mechanics - Part I: Theory", *J. Mech. Phys. Solids.*, **55**(6), 1274-1297. https://doi.org/10.1016/j.jmps.2006.11.003.

Gao, F., Zhu, J.G., Wang, T., Luo, Q.X., Wang, X.A. and Pan, L. (2025), "Experimental evidences on a unique critical state line for coarse-grained soil with different gradations in light of skeleton void ratio", *Geomech. Eng.*, **41**(5), 493-505. https://doi.org/10.12989/gae.2025.41.5.493.

Guo, W.L., Huang, Y.H., Fourie, A. and Wu, Y.L. (2019), "Mathematical model revealing the evolution of particle breakage and particle-size distribution for rockfill during triaxial shearing", *Eur. J. Environ. Civ. Eng.*, **25**(5), 893-908. https://doi.org/10.1080/19648189.2018.1552898.

Guo, W.L. and Chen, G. (2022), "Particle breakage and gradation evolution of rockfill materials during triaxial shearing based on the breakage energy", *Acta. Geotech.*, **17**(11), 5351-5358. https://doi.org/10.1007/s11440-022-01690-7.

Guo, W.L., Song, D.Q. and Li, X.M. (2024), "Unified model of critical state line for rockfill material with and without considering particle breakage", *Acta. Geotech.*, **19**, 2273-2291. https://doi.org/10.1007/s11440-023-02095-w.

Hardin, B.O. (1985), "Crushing of soil particles", *J. Geotech. Eng.*, **111**(10), 1177-1192. https://doi.org/10.1061/(ASCE)0733-410(1985)111:10(11
77).

Indraratna, B., Lackenby, J. and Christie, D. (2005), "Effect of confining pressure on the degradation of ballast under cyclic loading", *Géotechnique.*, **55**(4), 325-328. https://doi.org/10.1680/geot.2005.55.4.325.

Kiana, A.R.T., Zakerib, J.A. and Sadeghi, J. (2018), "Experimental investigation of effects of sand contamination on strain modulus of railway ballast", *Geomech. Eng.*, **14**(6), 563-570. https://doi.org/10.12989/gae.2018.14.6.563.

Jia, Y.F., Xu, B., Chi, S.C., Xiang, B. and Zhou, Y. (2017), "Research on the particle breakage of rockfill materials during triaxial tests", *Int. J. Geomech.*, **17**(10), 04017085. https://doi.org/10.1061/(ASCE)GM.1943-5622.0000977.

Lade, P.V., Yamamuro, J.A. and Bopp, P.A. (1996), "Significance of particle crushing in granular materials", *J. Geotech. Eng.*, **122**(4), 309-316. https://doi.org/10.1061/(ASCE)0733-9410(1996)122:4(309).

Lee, K.L. and Farhoomand, I. (1967), "Compressibility and crushing of granular soil in anisotropic triaxial compression", *Can. Geotech. J.*, **4**(1), 68-86. https://doi.org/10.1139/t67-012.

Li, K.P., Chen, S.H., Zhao, P. and Pei, R.P. (2024), "Theoretical and numerical simulation analysis of the control effect of isolation piles on surface settlement induced by foundation pit excavation", *Geomech. Eng.*, **39**(3), 227-240. https://doi.org/10.12989/gae.2024.39.3.227.

Li, X., Liu, J.K. and Li, J.Z. (2022), "Fractal dimension, particle shape, and particle breakage analysis for calcareous sand", *Bull. Eng. Geol. Environ.*, **81**(3), 116. https://doi.org/10.1007/s10064-022-02585-3.

Ma, C.K., Zhang, C., Chen, Q.L., Pan, Z.K. and Ma, L. (2021), "On the effect of void ratio and particle breakage on saturated hydraulic conductivity of tailing materials", *Geomech. Eng.*, **25**(2), 159-170. https://doi.org/10.12989/gae.2021.25.2.159.

Marsal, R.J. (1967), "Large scale testing of rockfill materials", *J. Soil. Mech. Found. Div.*, **93** (2), 27-43. https://doi.org/10.1061/JSFEAQ.0000958.

McDowell, G.R., Bolton, M.D. and Robertson, D. (1996), "The fractal crushing of granular materials", *J. Mech. Phys. Solids.*, **44**(12), 2079-2102. https://doi.org/10.1016/S0022-5096(96)00058-0.

McDowell, G.R. and Bolton, M.D. (1998), "On the micromechanics of crushable aggregates", *Géotechnique.*, **48**(5), 667-679. https://doi.org/10.1680/geot.1998.48.5.667.

McDowell, G.R. and Daniell, C.M. (2001), "Fractal compression of soil", *Géotechnique.*, **51**(2), 173-176. https://doi.org/10.1680/geot.2001.51.2.173.

Muir Wood, D. and Maeda, K. (2008), "Changing grading of soil: effect on critical states", *Acta. Geotech.*, **3**(1), 3-14. https://doi.org/10.1007/s11440-007-0041-0.

Nakata, Y., Hyde, A.F.L., Hyodo, M. and Murata, H. (1999), "A probabilistic approach to sand particle crushing in the triaxial test", *Géotechnique.*, **49**(5), 567-583. https://doi.org/10.1680/geot.1999.49.5.567.

Nhua, T.Q., Nipawan, K., Warakorn, M., Bunpoat, K. and Thawatchai, C. (2024), "Behavior of seepage in earth dams through complex foundations using three-dimensional finite

element method", *Geomech. Eng.*, **39**(3), 273-282. https://doi.org/10.12989/gae.2024.39.3.273.

Salim, W. and Indraratna, B. (2004), "A new elastoplastic constitutive model for coarse granular aggregates incorporating particle breakage", *Can. Geotech. J.*, **41**(4), 657-671. https://doi.org/10.1139/t04-025.

Shi, J.W., Chen, Y.H., Kong, G.Q., Lu, H., Chen, G. and Shi, C. (2024), "Deformation mechanisms of an existing pipeline due to progressively passive instability of tunnel face: Physical and numerical investigations", *Tunn. Undergr. Sp. Tech.*, **150**, 105822. https://doi.org/10.1016/j.tust.2024.105822.

Shi, J.W., Zhong, X.C., Lu, H., Ni, X.D. and Shi, C. (2025), "Influence of joint stiffness on three-dimensional deformation mechanisms of pipeline under tunnel active face instability", *Can. Geotech. J.*, **62**, 1-16. https://doi.org/10.1139/cgj-2024-0092.

Shi, K., Zhu, F. and Zhao, J.D. (2022), "Multi-scale analysis of shear behaviour of crushable granular sand under general stress conditions", *Géotechnique*., **74**(5), 443-460. https://doi.org/10.1680/jgeot.21.00412.

Von Rittinger, P.R. (1867), "Zweiter nachtrag zum lehrbuch der aufbereitungskunde", Berlin: Verlag, Ernst & Korn.

Wadell, H. (1932), "Volume, shape, and roundness of rock particles", *J. Geol*., **40**(5), 443-451.

Wang, T., Tang, C.S., Liu, W.J., Cheng, Q., Shen, Z.T. and Pan, X.H. (2024a), "Insight into the initiation and propagation mechanism of desiccation cracking in clayey soil from DEM simulations", *Comput. Geotech*., **175**, 106694. https://doi.org/10.1016/j.compgeo.2024.106694.

Wang, T., Wautier, A., Tang, C.S. and Nicot, F. (2024b), "3D DEM simulations of cyclic loading-induced densification and critical state convergence in granular soils", *Comput. Geotech*., **173**, 106559. https://doi.org/10.1016/j.compgeo.2024.106559.

Wang, T., Tang, C.S., Liu, W.J., Cheng, Q. and Zeng, Z.X. (2025), "Process and mechanism of soil desiccation cracking triggered by surface defects based on DEM modeling", *J. Geophys. Res. Earth Surf.*, **130**(5), e2024JF008121. https://doi.org/10.1029/2024JF008121.

Wang, X., Cui, J. and Wang, W. (2024), "Dilatancy behaviors of calcareous sand considering particle breakage", *Bull. Eng. Geol. Environ*., **83**(4), 1-24. https://doi.org/10.1007/s10064-024-03618-9.

Wang, X.Z., Shan, H.G., Meng, Q.S. and Zhu, C.Q. (2020), "Factors affecting particle breakage of calcareous soil retrieved from South China Sea", *Geomech. Eng.*, **22**(2), 173-185. https://doi.org/10.12989/gae.2020.22.2.173.

Wang, Z.N., Wang, G. and Ye, Q.G. (2020), "A constitutive model for crushable sands involving compression and shear induced particle breakage", *Comput. Geotech*., **126**, 103757.
https://doi.org/10.1016/j.compgeo.2020.103757.

Xiao, Y., Yuan, Z.X., Lv, Y.R., Wang, L.J. and Liu, H.L. (2018), "Fractal crushing of carbonate and quartz sands along the specimen height under impact loading", *Constr. Build. Mater*., **182**, 188-199. https://doi.org/10.1016/j.conbuildmat.2018.06.112.

Xiao, Y., Wang, C.G., Wu, H.R. and Desai, C.S. (2021), "New simple breakage index for crushable granular soils", *Int. J. Geomech*., **21** (8), 04021136. https://doi.org/10.1061/(ASCE)GM.1943-5622.00020.

Xiao, Y., Sun, Y., Zhou, W., Shi, J.Q. and Desai, C.S. (2022a), "Evolution of particle shape produced by sand breakage", *Int. J. Geomech*., **22**(4), 04022003. https://doi.org/10.1061/(ASCE)GM.1943-5622.0002333.

Xiao, Y., Ling, Y.Y., Shi, J.Q., Sun, Y. and Liu, H.L. (2022b), "Breakage and morphology of sands in drained shearing", *Int. J. Geomech*., **22**(9), 04022140. https://doi.org/10.1061/(ASCE)GM.1943-5622.000252.

Yang, Z.Y. and Juo, J.L. (2001), "Interpretation of sieve analysis data using the box-counting method for gravelly cobbles", *Can. Geotech. J.*, **38**(6), 1201-1212. https://doi.org/10.1139/t01-052.

Yu, F.W. (2017), "Characteristics of particle breakage of sand in triaxial shear", *Powder. Technol*., **320**, 656-667. https://doi.org/10.1016/j.powtec.2017.08.001.

Yu, F.W. (2018), "Particle breakage in triaxial shear of a coral sand", *Soils. Found*., **58**(4), 866-880. https://doi.org/10.1016/j.sandf.2018.04.001.

Zeng, K.F. and Liu, H.B. (2023), "Effect of particle size distributions on the mechanical behavior and particle breakage of coral sands", *Granul. Matter*., **25**(3), 44. https://doi.org/10.1007/s10035-023-01334-x.

Zhang, J.R., Hua, C., Luo, M.X. and Zhang, B.W. (2020), "Behavior of particle breakage in calcareous sand during drained triaxial shearing", *Chin. J. Geotech. Eng*., **42**(9), 1593-1602. https://doi.org/10.11779/CJGE202009003.

Zhou, L.L. and Zhang, X. (2016), "Numerical investigations on breakage behaviour of granular materials under triaxial stresses", *Geomech. Eng*., **11**(5), 639-655. https://doi.org/10.12989/gae.2016.11.5.639.

Zhu, J.G., Guo, W.L., Wen, Y.F., Yin, J.H. and Zhou, C. (2018), "New gradation equation and applicability for particle-size distributions of various soils", *Int. J. Geomech*., **18**(2), 04017155. https://doi.org/10.1061/(ASCE)GM.1943-5622.000108.

GC